

**A FULLY IMPLANTABLE, MINIATURIZED RFID PLATFORM FOR  
NEUROSURGICAL BIOMEDICAL DEVICES**

An Undergraduate Research Scholars Thesis

by

SERGIO SEBASTIAN PINEDA

Submitted to the Undergraduate Research Scholars program at  
Texas A&M University  
in partial fulfillment of the requirements for the designation as an

UNDERGRADUATE RESEARCH SCHOLAR

Approved by Research Advisor:

Dr. Sung Il Park

May 2018

Major: Electrical Engineering

# TABLE OF CONTENTS

	Page
ABSTRACT.....	1
ACKNOWLEDGMENTS .....	2
ACRONYMS.....	3
CHAPTER	
I. INTRODUCTION .....	4
Background and Motivation .....	4
Approach.....	7
II. DESIGN AND TESTING METHODOLOGY .....	9
Design and Architecture .....	9
Fabrication and Assembly.....	16
Testing Methodology .....	17
III. RESULTS .....	19
Computational Simulations.....	19
Inductance Measurements.....	20
IV. DISCUSSION AND CONCLUSIONS .....	22
Technological Challenges.....	23
Limitations of Current Design .....	23
Future Directions .....	24
REFERENCES .....	26

## **ABSTRACT**

A Fully Implantable, Miniaturized RFID Platform for Neurosurgical Biomedical Devices

Sergio Sebastian Pineda  
Department of Electrical and Computer Engineering  
Texas A&M University

Research Advisor: Dr. Sung Il Park  
Department of Electrical and Computer Engineering  
Texas A&M University

Hydrocephalus occurs when excessive quantities of cerebrospinal fluid (CSF) accumulate in the ventricles. Current treatment of the condition involves implanting a ventricular shunt, composed of an inflow catheter originating at the site of the obstructed ventricle, a valve, and an outflow catheter that drains the excess fluid into the peritoneal cavity where it can be safely reabsorbed or excreted. This method of treatment is crude and subject to many complications including, but not limited to, infection, blockage, and over-draining. Therefore, the flow of CSF out of the ventricles and into the abdomen must be carefully monitored. Unfortunately, there is currently no effective and non-invasive means of doing so.

Here we present the design and partial integration of a prototype for a wireless, fully implantable, miniaturized RFID-based device for monitoring and recording the functional state of a ventricular shunt. The purpose of this device is to provide a minimally-invasive and robust method for digitally interrogating shunt function. Such a platform would, ideally, allow for real-time, wireless monitoring which will serve to inform the patient and their care providers of abnormalities in shunt performance and allow them to take the appropriate measures before further complications can occur.

## **ACKNOWLEDGEMENTS**

I would like to thank Dr. Sung Il Park for his guidance, and for providing me with the resources necessary to undertake this project. I would also like to thank Woo Seok Kim and Ruida Liu for assisting me with simulations, fabrication, and troubleshooting, and Dr. Clint Morgan for providing us with his medical expertise.

## ACRONYMS

MEMS	Microelectromechanical Systems
IC	Integrated Circuit
CSF	Cerebrospinal Fluid
NFC	Near-Field Communication
RFID	Radio Frequency Identification
RF	Radio Frequency
PLA	Polylactic Acid
PDMS	Polydimethylsiloxane
DC	Direct Current
HFSS	High-Frequency Structure Simulator

# CHAPTER I

## INTRODUCTION

Advances in semiconductor microfabrication techniques, low-power ICs, wireless power transmission systems, and MEMS sensors have ushered in a new era for implantable biomedical device technology. Such systems have been developed and introduced in the laboratory setting for medical research purposes ranging from optical neuromodulation to testing next-generation medical sensors for transcranial applications. There has been much exploration into the possibility of translating this type of technology for clinical applications such as wirelessly rechargeable pacemakers and spinal nerve stimulators. In this paper, we propose a clinical implementation of this technology for facilitating the management of hydrocephalus.

### **Background and Motivation**

Hydrocephalus is a medical condition characterized by the accumulation of CSF in the ventricles of the brain, resulting in their enlargement and causing intracranial hypertension. This accumulation can stem from multiple conditions. Most prevalent are the obstruction of CSF flow out of, or between the ventricles, a failure to reabsorb sufficient quantities of the fluid, or the overproduction of CSF. The two obstruction-induced forms of the condition are called communicating or non-communicating hydrocephalus, depending on the type of obstruction. Any variation of the condition in which CSF is still allowed to flow between the ventricles is described as communicating, this includes the scenario in which CSF cannot be properly reabsorbed into the subarachnoid space despite there being no apparent blockage of CSF out of the ventricles. Non-communicating hydrocephalus refers to the case where CSF flow out of the ventricular system is

physically blocked. The blockage need not be located near the ventricles, as in the case of spina bifida, in which an obstruction in the lower spine can induce hydrocephalus.

Hydrocephalus is generally congenital, with an occurrence frequency of approximately 1.5 of every 1000 births. However, forms of the condition known as normal pressure hydrocephalus and hydrocephalus *ex vacuo* can be acquired as a consequence of head trauma, infection, cancer, and even from neurodegenerative and neuropsychiatric diseases that are accompanied by brain atrophy. Congenital hydrocephalus often results in an infant experiencing a rapid and noticeable increase in head circumference shortly after birth, and can be easily diagnosed through a variety of medical imaging modalities. In older patients, and especially so in adults with an acquired form of the condition, the diagnosis is more difficult as the symptoms are non-specific and can be affiliated with a multitude of neurological conditions. Common symptoms are a product of the surrounding brain tissue being compressed by the expanding ventricles and include, but are not limited to, headaches that vary drastically in severity, seizures and convulsions, vomiting, motor impairment, and cognitive impairment [1][2].

At this time, the causes of most forms of congenial hydrocephalus are unknown. There is currently no cure for congenial or most forms of acquired hydrocephalus, and the condition is fatal if left untreated. Treatment options are limited and usually involve maintaining the intracranial pressure at a safe level through surgical approaches. The most common of these approaches is the implantation of a ventricular shunt and catheter that diverts the excess CSF from the ventricular system and releases it into another area of the body where it can be reabsorbed; a typical release target is the peritoneal cavity [3]. A patient will have such a shunt system inserted shortly after birth, which will be surgically removed and replaced as the patient outgrows it. Once they have reached adulthood, the patient will ideally be left with a permanent shunt that will

continue to maintain an acceptable intracranial fluid pressure for the remainder of their life. The daily production of CSF in a typical adult is estimated to be between 500-700 mL per day, and the ventricular system has the capacity to hold approximately 125-150 mL at any given time [4], hence these shunts are expected to handle a fairly large and continuous amount of fluid quite reliably. In practice, however, this does not happen and these shunts are extremely susceptible to failure. Blockage, infection, disconnection, and over draining are examples of common complications that would require immediate surgical intervention. Even if these shunts are well maintained and infection or blockage does not occur, they will still degrade over time. Cheatle et al. [5] observed that under normal operating conditions fluid resistance in standard silicone shunt catheters increases over time. When failure occurs, standard procedure is to surgically remove and replace the shunt as soon as possible.

Since these shunts have such a high failure rate, physicians take care to monitor their status as best as they can, though the amount of information regarding shunt function that they can retrieve is limited. Patients are often asked to carry with them a card detailing shunt information like a record of inspection and surgical history pertaining to the shunt. However, unless this vital information is taken to the same care provider where the information has context, it may be useless. Shunt failure is difficult to identify and is usually diagnosed when neurological episodes involving the aforementioned symptoms occur. When these shunts fail, the patient is at risk of further damage to brain tissue, and therefore there exists a demand for a system capable of detecting shunt failure prior to the appearance of these symptoms, allowing the patient's care providers to preemptively intervene before further medical complications arise.

Hydrocephalus is particularly problematic in developing countries, where access to shunts is extremely limited, both by cost and medical infrastructure [6]. Even in the United States the cost



of a ventricular shunt is astronomical [7], and therefore it is not only important to be able to predict shunt failure, but ideally have it done quickly and precisely enough to minimize damage to the shunt (in cases where damage to the shunt itself is not the source of failure) and potentially be able to clean and reuse it.

## **Approach**

In an effort to satisfy the demand for such a system, we sought to develop a wireless and implantable sensing and data logging platform that can provide a patient with such information by detecting anomalies in catheter performance through deviations from standard operating parameters, such as statistically significant changes in intra-catheter flow rate and fluid pressure. We also proposed integrating a “shunt tag” in the same system that would replace the shunt information and history card by storing a digital copy of this crucial information on static memory that could be wirelessly retrieved and updated with ease. We elected to use RFID, a widespread, short distance, and wireless communication standard as the basis of the device’s wireless capabilities. RFID was chosen for its simplicity, impressively low cost, ease of integration with third-party systems, and its ability to transmit both information and power at distances suitable for this application. RFID-based devices can also be safely implanted in deep tissues since the amount of power transmitted poses no harm.

To facilitate the mass production and maximize the accessibility of such a platform, we made every effort to use cost-effective fabrication techniques and low-cost, off-the-shelf hardware for the development of this platform. We designed the communication interface of the device so that we can easily transition to an NFC-based platform in a future iteration. This would allow us to make real-time measurements, supply power, and retrieve clinically pertinent data for immediate transmission using a low-cost NFC reader or even a smart phone. Giving the patient

the ability to assess shunt function on-the-fly and send status updates to their care providers would ensure that immediate medical intervention will occur in the event of a malfunction before neurological symptoms arise.

## CHAPTER II

### DESIGN AND TESTING METHODOLOGY

#### Design and Architecture

The device architecture is quite simple, as can be seen from the circuit schematic shown in **Figure 1**. The primary components of this apparatus are an antenna, an RFID sensor tag and data-logger IC (MLX90129, Melexis, Belgium), an instrumentation amplifier, (INA333, Texas Instruments, USA), a miniature pressure sensor die (P162, Amphenol Advanced Sensors, USA), and a pair of custom ‘fluid switches’ composed of a single, long pass-through fluid channel with five smaller intersecting vertical channels that allow the fluid to exert a force on the sensor die and contact four metal pads situated underneath. The MLX90129 also functions as a power supply for the rest of the hardware and receives input from the sensors. The MLX90129 is, in turn, supplied power through induction by the coil that surrounds the device.

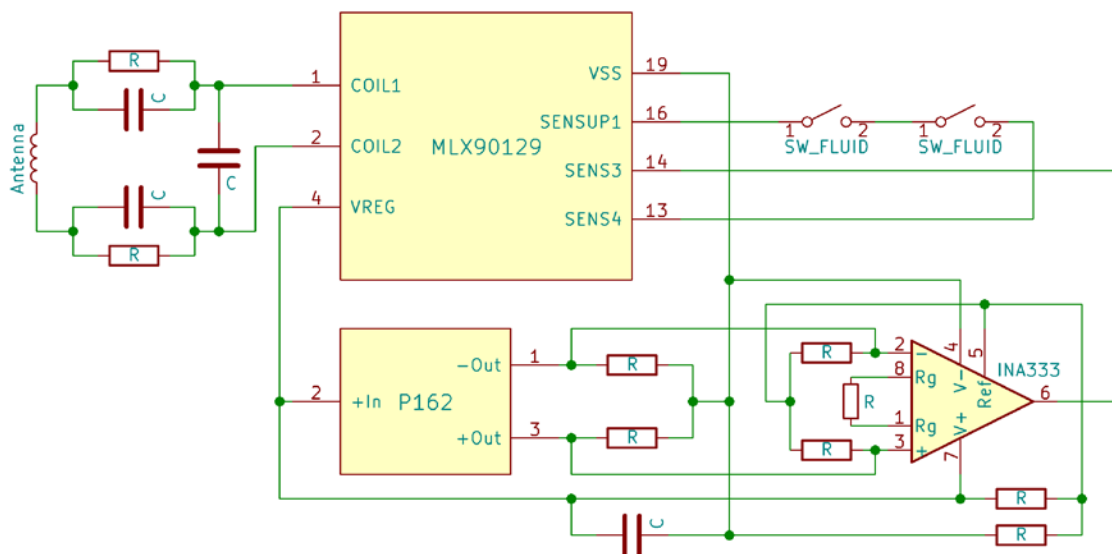


**Figure 1. Circuit schematic of device.**

The same coil functions as an RFID antenna necessary for the transmission of sensor data between the device and an external transmitter via the MLX90129.

In order to maximize device longevity and biocompatibility, we opted for a flexible circuit design that could better tolerate the shearing and bending forces that chronic implants are typically subjected to. The antenna, traces, and component mounting pads (**Figure 2**) were etched from a copper laminate on a polyimide substrate (Pyrallux, DuPont, USA). A trace width of 100  $\mu\text{m}$  and an antenna width of 125  $\mu\text{m}$  were chosen for fast and stable wet-etching, though more sophisticated etching techniques could be used to easily fabricate thinner traces. The antenna (shown in green) is roughly 2  $\times$  2 cm. The device is enclosed in PDMS and isolated from surrounding tissues and fluids.

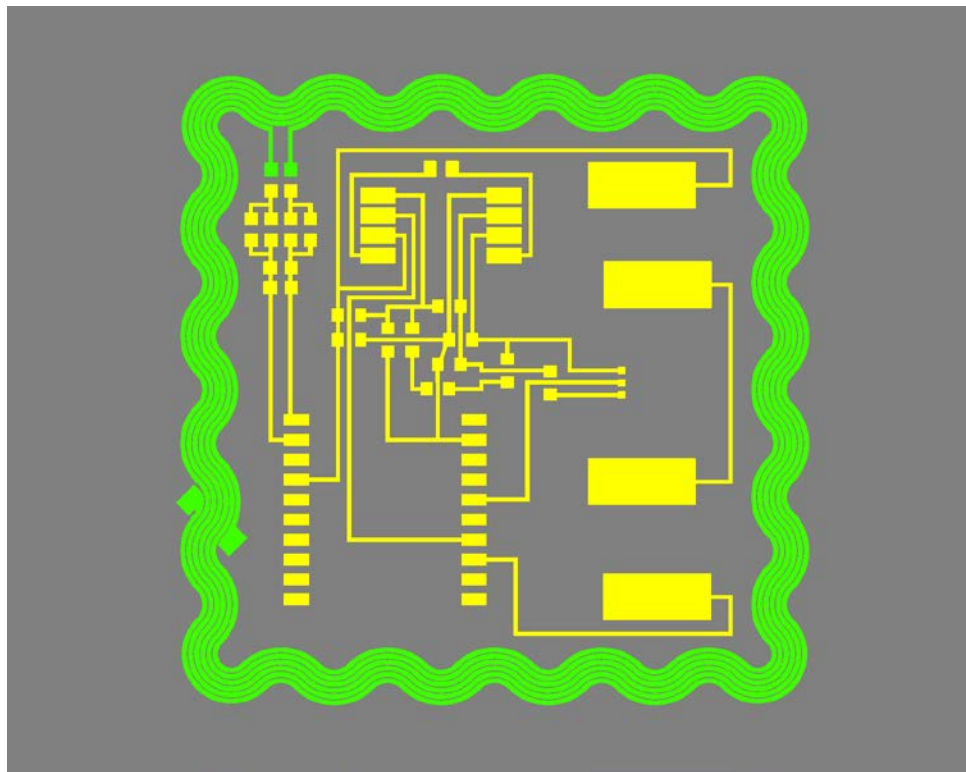


**Figure 2. Copper footprint of apparatus.** Antenna shown in green. Solder pads and traces shown in yellow.

The assembled apparatus rests entirely on the Pyralux film which is then attached to a flexible ferrite sheet for the purpose of increasing antenna inductance, and by extension, energy-harvesting efficiency. The square-serpentine shape of the antenna was chosen to ease the transition to a stretchable design in a future iteration. The channel used here was 3D-printed and constructed from PLA. PLA, however, was chosen for prototyping purposes only and cannot be used in clinical implementation because it is biodegradable and will break down into lactic acid several months [8]. The ends of the 25 mm long channel (**Figure 3**) connect two disjoint segments of the distal catheter, allowing CSF to pass through the device while taking measurements.

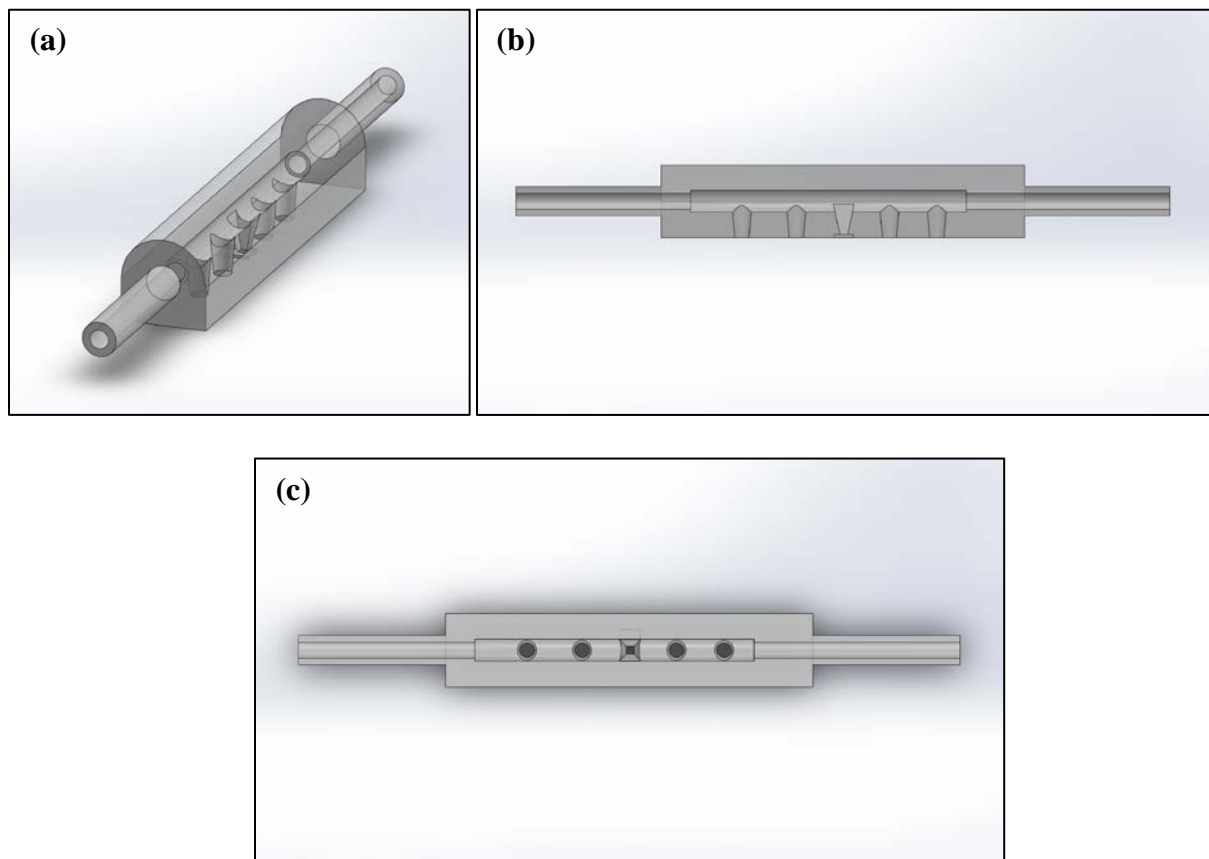


**Figure 3. Diagram of fluid channel.** (a) Isometric view. (b). Cross-sectional side view. (c). Cross-sectional top view.

The diameter of the channel is 1 mm, the same as the diameter of a standard silicone distal catheter used in ventricular shunt systems, so that the CSF may flow unobstructed and without experiencing a change in pressure at the site of measurement. The long channel has five much smaller channels intersecting it perpendicularly. The vertical channel located at the center in **Figure 3(a)** serves the purpose of allowing the CSF to put pressure on the pressure sensor die. The remaining four protrusions terminate at conductive gold plates to form the two ‘fluid switches’. A rendering of the fully assembled device, sans the PDMS enclosure, is shown in **Figure 4**.

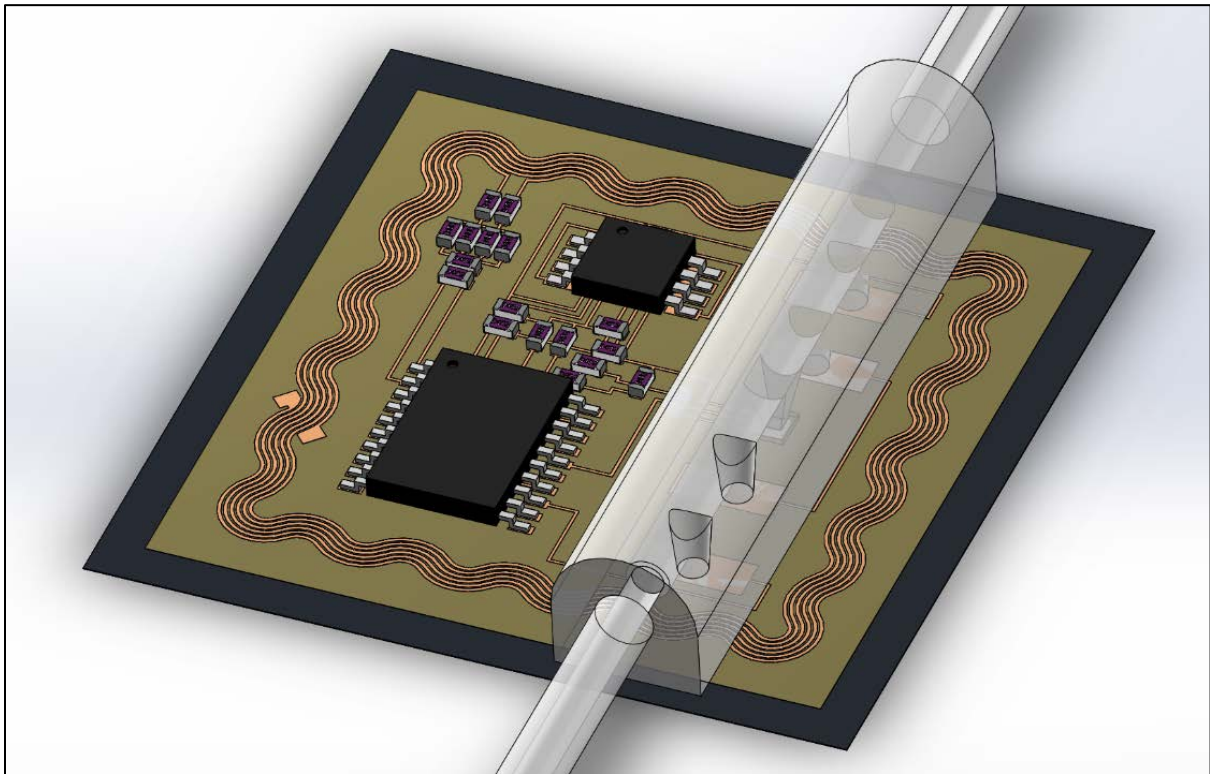


**Figure 4. Rendering of fully-assembled platform.** Excess polyimide and ferrite film around antenna shown to emphasize device topology. Material outside the antenna boundary would typically be cut away. PDMS enclosure omitted for visibility.

The entire apparatus is encapsulated in PDMS, a highly biocompatible silicon-based organic polymer that is widely used in medical implants. As mentioned, the pads below the fluid

channel make direct contact with the CSF inside the channel. Copper is corrosive and toxic, and so it cannot be allowed to make direct contact with bodily fluids, both to prevent toxicity and to maintain the structural integrity of the device [9]. For this reason, a thin layer of gold, which is non-corrosive and biocompatible, must be deposited atop these pads to prevent corrosion.

#### *Obstruction Detection Mechanism*

A flowmeter of sufficiently small size and power consumption, and sufficiently high resolution is not available on the market, to our knowledge, and proposed designs found in literature did not conform to the constraints imposed by our design criteria or the device's operational environment. As a result, we had to, for now, abandon the idea of a precision flow sensing platform and opted for a design that granted reduced functionality, but was still capable of producing clinically significant measurements. We designed a system that could detect total catheter obstruction above or below the location of the device along the distal catheter. This scheme functions by way of two 'sensors' that generate binary outputs depending on the type of obstruction. Any combination of these two outputs represents one of four possible cases. **Figure 5** shows the design of the sensing mechanism.

The 3D-printed fluid channel (semi-transparent gray component in **Figure 4**) is connected in between two segments of the distal catheter. As stated previously, the pass-through channel has five vertical projections intersecting the main, 25 mm long tube. The square-shaped projection in the middle allows fluid to stimulate the MEMS pressure sensing die situated underneath. **Table 1** shows the possible outputs and their interpretations. All cases that fall outside of 'normal operation' will require some form of intervention. Under normal operation, the fluid force on the die is usually undetectable, but in the event of distal obstruction, the pressure becomes sufficient to generate a voltage that will saturate the output of the amplifier.

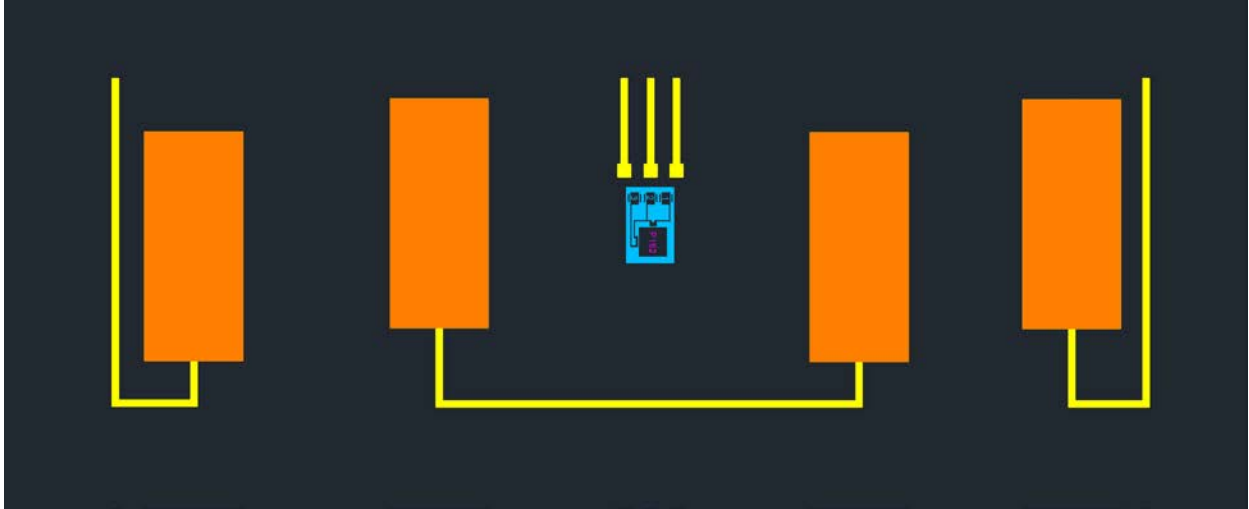


**Figure 5. Dual sensor design.** The obstruction detection scheme combines a miniature pressure sensor die and four conductive pads which are shorted in the presence of CSF. The four small outer vertical channels of the pass-through channel allow CSF to come in contact with each of the four large gold pads (shown in orange). The central square channel allows the CSF to exert pressure on the P162 pressure sensing die (shown in blue). Copper traces are shown in yellow.

Table 1. Evaluation of shunt obstruction from sensor outputs.

<b>Voltage at SENS3 (Pressure)</b>	<b>Voltage at SENS4 (Fluid)</b>	<b>Shunt State</b>
LOW	LOW	<b>Obstruction (Proximal)</b>
HIGH	LOW	<b>Sensor Error</b>
LOW	HIGH	<b>Normal Operation</b>
HIGH	HIGH	<b>Obstruction (Distal)</b>

This will be read as a HIGH input signal at SENS3 (on the MLX90129). The four remaining protrusions form a pair of ‘switches’ that allow current to flow from SENSUP1 to SENS4



(generating a HIGH signal) if there is a conductive fluid (such as CSF) in the channel to bridge the gaps between the pads. In the event of proximal obstruction, CSF will drain from the channel within several hours to a day, resulting in an open circuit. SENS3 will therefore receive a LOW signal.

The choice of a four pad/two switch design rather than two pad/one switch stemmed from the possibility that a small amount of CSF could, under the right circumstances, remain in place despite proximal obstruction, possibly due to increased abdominal pressure that prevents complete evacuation of the channel. This would still allow current to flow between the conductors, even if most of distal tubing empties, and generate a HIGH signal at SENS4 even though there is blockage. The two gap design means that a greater amount of fluid would have to remain in the channel for some period of time in order to generate a false positive. The output signal of the pressure sensor die is on the order of microvolts, so an INA333 instrumentation amplifier, configured for a gain of 1000, couples the sensor output to SENS3. The high gain ensures that the output saturates when the sensor is subjected to abnormally high pressure and effectively converts the analog output from the die to a digital input at the data-logging IC.

#### *Communication and Power Transmission*

We elected to use an RFID-based system for communication and power transmission between the device and an off-the-shelf transmitter. RFID is an exceptionally common and simple communication system for short-range data and power transmission. It is suitable for bilateral communication between low-power, portable devices, and specifies an operating frequency of 13.56 MHz, which has the advantage of easily penetrating non-conducting media. It has also been shown that this frequency interacts weakly and safely with biological tissues [10]. These properties make the use of RFID optimal for our purposes. We designed the device to be passively powered,

so the antenna is the exclusive source of power. Although the integration of a small battery would improve device performance and allow greater flexibility with regards to the selection of data-logging and sensing hardware, we wanted the device to effectively be part of the catheter and be simultaneously implanted and replaced during shunt revisions. A battery could potentially set a limit on the highly variable lifetime of a catheter. We are, however, considering the addition of an inductively rechargeable battery in future iterations. The “antenna” used in our design is an inductor coil rather than a microstrip antenna since the desired operating range is quite short and will require minimal modification when we transition to an NFC-based design in a future iteration.

### **Fabrication and Assembly**

The flexible antenna, solder pads, and traces of the device were fabricated using a wet-etching process. Positive photoresist was used for the photolithography phase to create the device footprint from a copper laminate adhered to a polyimide substrate (Pyralux). Widths of 125  $\mu\text{m}$  and 100  $\mu\text{m}$  were chosen for the antenna and traces, respectively, and the spacing between the windings of the antenna was 75  $\mu\text{m}$ . The entire copper footprint of the device has a uniform height of 5  $\mu\text{m}$ . This height was chosen because it can be reliably etched using a wet process. The solder pads of all passive surface-mounted components conform to the SMD 0201 dimensions (0.6 mm  $\times$  0.3 mm). A gold layer of equal thickness is deposited atop the four pads situated beneath the pass-through channel using DC sputtering. After fabrication, the components are hand-soldered to the pads, with the exception of the pressure sensor die, which is to be wire bonded to the appropriate pads. The device is then fixed atop a 100  $\mu\text{m}$  thick flexible ferrite sheet to increase antenna inductance by a factor of 3. The die should not make direct contact with fluids, so a thin protective coating must be placed over the pressure die to prevent damage to the die surface. The pass-through channel in this prototype was 3D-printed using PLA at a 300  $\mu\text{m}$  resolution. As

stated, PLA is biodegradable and so a different biocompatible material must be chosen should the device ever see clinical use. The pass-through channel is attached to the copper-polyimide film using a USP Class VI-compliant adhesive. The entire device, with the exception of the channel's ports, is encapsulated in PDMS. The two segments of the distal catheter are attached at the exposed ports and sealed.

### **Testing Methodology**

Due to logistical issues and the unavailability of specific fabrication equipment necessary to build some of the necessary components, we were unable to produce a complete assembly of the device for testing. We were, however, able to fabricate the antenna and both computationally and physically characterize its performance. Computational simulations of the RF characteristics of the device and validation of the impedance matching network were done in HFSS (Ansys, USA). The data-logging and energy-harvesting IC was modeled as a 75 pF capacitor for impedance matching purposes, in accordance with the model given by the datasheet. After fabrication, inductance measurements for the antenna, with and without the ferrite film, were taken using a network analyzer. Should we be able to manufacture the pass-through channel, the proposed characterization of the sensing mechanism would consist of varying and obstructing the flow of a saline solution through a real catheter connected to the channel using a syringe pump. Measurements taken via the data-logging IC, under DC power, would be used to assess the validity of the cases given in **Table 1** for determining shunt status. The same experiment would be repeated with the fully integrated system under RF power. The flow rate range imposed by the syringe pump should mimic that of CSF under varying conditions.

After fabrication and assembly, the device is to be tested in tissue. Our proposed method for characterizing the performance of the finalized device is to integrate it into a real shunt system

and implant it in a cadaver. This would allow us to test the wireless energy-harvesting and data transmission performance of the device in a realistic operating environment. We have yet to design an experiment to evaluate device performance and degradation over the lifetime of the ventricular shunt.

## CHAPTER III

### RESULTS

#### Computational Simulations

**Figure 6** shows the results of the HFSS simulations for the S11 parameter of the antenna, including the impedance matching network and data-logging IC, without the ferrite sheet. The impedance matching network was simulated using the closest standard SMD capacitor and resistor values, which were the same that were used in assembly. The resonant frequency of the device in simulation was 13.95 MHz, which is sufficiently close to the target frequency of 13.56 MHz.

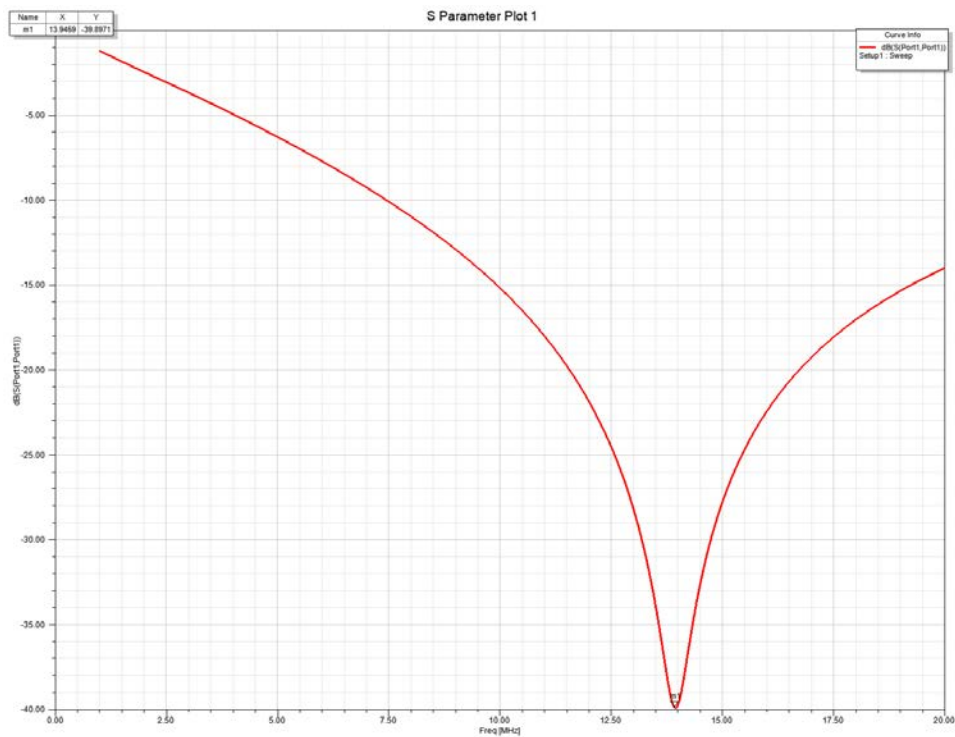


**Figure 6. Plot of S11 simulation on HFSS.** Frequency response plot of the S11 (reflection) parameter for the impedance-matched antenna shows a minimum (resonance frequency) at 13.9459 MHz

## Inductance Measurements

**Figure 7(a,b)** shows the Smith chart measurements taken with a network analyzer on the fabricated antenna. The real inductance in both cases varies slightly from this measurement due to parasitic capacitance introduced by the connector. Calculation of the real inductance yields a value of 3.72  $\mu\text{H}$  for the antenna with an air core, and 10.37  $\mu\text{H}$  with the ferrite sheet. The shunt tag function was trivially implemented as the MLX90129 already included such a feature. This feature is independent of the rest of the device design and could be just as easily implemented using any similar RFID chip.

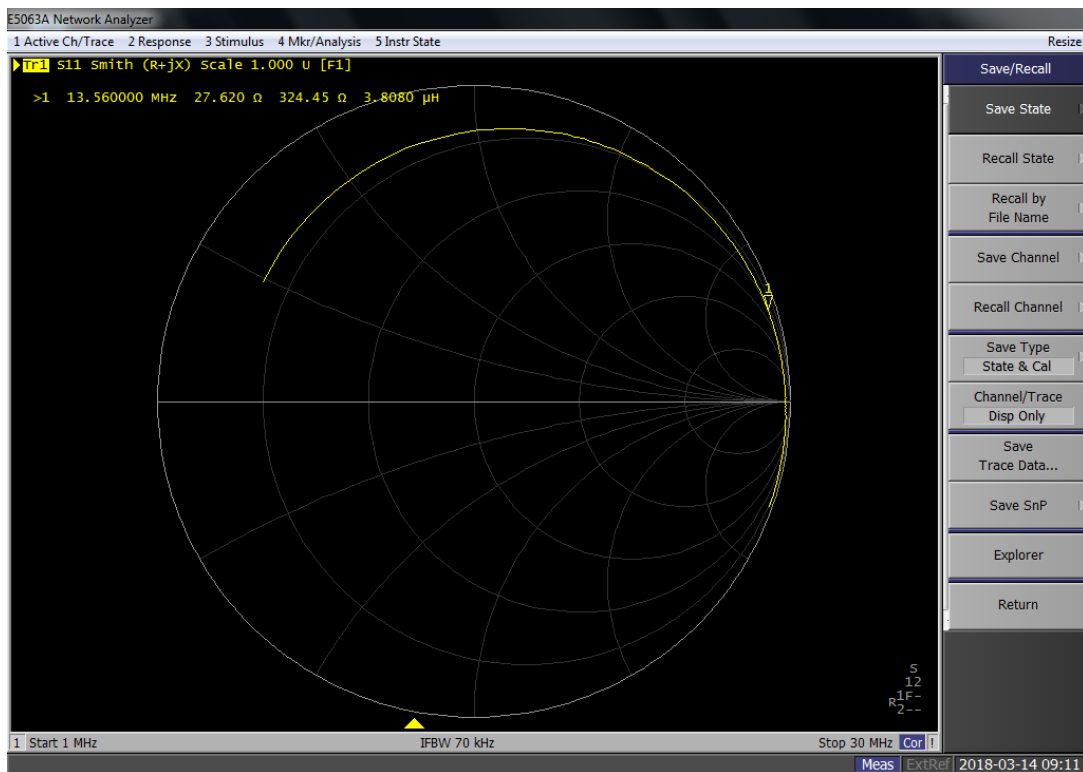


**Figure 7(a).** Inductance measurement of air core antenna. Network analyzer-generated Smith chart for the air core antenna showing an inductance of 3.808  $\mu\text{H}$  and a series coil resistance of 27.620  $\Omega$  at 13.56 MHz.

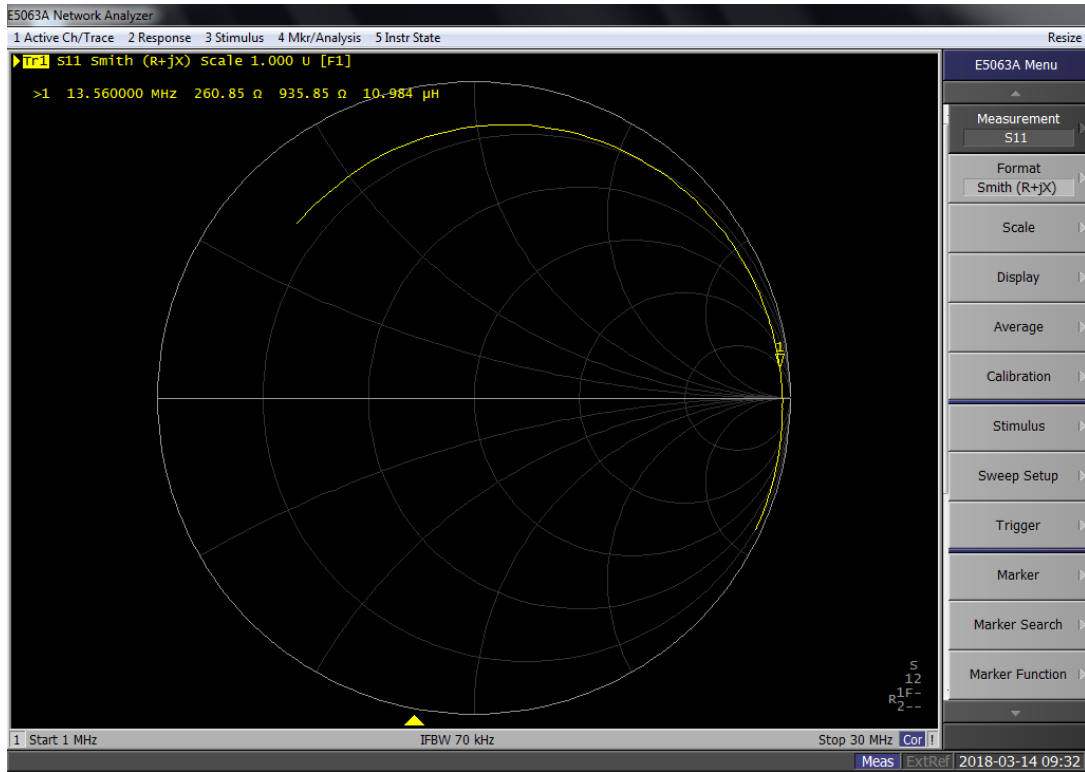


**Figure 7(b). Inductance measurement of ferrite core antenna.** Network analyzer-generated Smith chart for the ferrite core antenna showing an inductance of 10.984  $\mu\text{H}$  and a series coil resistance of 260.85  $\Omega$  at 13.56 MHz.

The use of ferrite results in a significant increase in the series resistance of the coil, which reduces the Q factor of the antenna by about a factor of 10.

## CHAPTER IV

### DISCUSSION AND CONCLUSIONS

Unfortunately, we were unable to create a fully assembled prototype of our platform at the time of this writing. However, we plan to construct and test the completed apparatus in the coming weeks. Previous attempts at constructing miniature, flexible devices for measuring intracranial pressure near the brain have been successful in animal models [11], and patents have been filed for other devices that make similar measurements in humans [12], but none have so far seen clinical use for a variety of reasons. The measurement of CSF flow at the ventricles does little to tackle the issue of shunt failure since such failure often happens further down the distal catheter, which is narrower than the proximal catheter. Since we are interested in the flow of CSF through the catheter, rather than at the ventricles, it makes more sense to take the measurement at the distal catheter. Similarly, an implantation procedure at the abdomen carries far less risk to the patient than inserting a measurement apparatus near the brain, but provides the same clinical information. The problem is that the development of a device that measures the flow or pressure at the distal catheter rather than near the cranium is more difficult, since the pressure at this site is weaker and more volatile. The flow and pressure of CSF outside the ventricles depends on the orientation of the patient, and at the catheter it is further affected by the exact positioning of the catheter, which is susceptible to motion, the type of catheter used, and any external mechanical forces that act on it. During the development of this platform, we identified a series of key challenges and limitations, some of which we were unable to address even theoretically. We were initially surprised that such a simple and essential device had not yet been developed, and these obstacles, we believe, are the reason.



## **Technological Challenges**

The foremost reason that we chose such an unconventional sensing mechanism to detect obstruction is the lack of a commercially available flow sensor with the necessary resolution, but which is also energy efficient enough to function under RF power without damaging biological tissue. We explored the possibility of utilizing a battery-powered flow sensor, but it was similarly challenging to find one with the performance characteristics, size, and form factor necessary for this application. We will continue to entertain the idea of a rechargeable battery-powered flowmeter in the future, provided that a suitable flow sensor can be fabricated, but currently this limitation does not justify the time and cost of incorporating a charge controller. Raj et al. [13] have proposed a similar platform with a novel flowmeter design, but it requires a wireless spectrometer and is not cost effective. Cost-effectiveness is imperative since not only is the device technically disposable, but the overwhelming majority of hydrocephalus cases happen in less developed regions where access to such medical devices is limited and cost plays a major role. Apigo et al. have proposed a type of differential flowmeter specifically designed for ventricular shunts that compares the pressure at two regions of the distal catheter using a looped design [14]. Our implementation, though rudimentary, should serve as a good starting point for a more advanced system, by at least providing information about shunt failure in the most extreme case, that being total obstruction.

## **Limitations of Current Design**

The most obvious limitation, as already mentioned, is the low sensitivity of the obstruction sensing mechanism. Currently, we would only be able to detect the most extreme case of shunt failure, where either the upper region of the catheter is completely blocked, allowing the CSF to drain from the channel after a period of time (on the order of several hours) as allowed by the

abdominal pressure of the stomach, or where obstruction below the channel is sufficient to allow a significant buildup of CSF in the tubing. In many cases, the rate of deterioration of the tubing, or the accumulation of debris that would cause an obstruction is slow enough that complications from lack of drainage could occur before the system detects a problem. The high amplification of the pressure sensor output mitigates this somewhat by increasing the likelihood that an event of this nature can be detected at the distal end, though we have not yet been able to verify that this will work. No such mechanism is in place to account for this scenario on the proximal side.

We addressed the problem of copper corrosion through the deposition of gold where the CSF and the copper pads make contact, but unfortunately there is still the issue of plaque buildup at these locations. Our group has, in previous projects, encountered the issue where gold conductors lose their conductivity after being exposed to bodily fluids, including CSF, for extended periods of time. Our model mimics CSF by using a saline solution, which is reasonable since CSF has roughly the same viscosity and density as water with some dissolved ionic species. However, CSF also carries some protein content that, although negligible when examining its fluidic properties, can accumulate on the surface of gold, creating a plaque that reduces or blocks the flow of current from the fluid to the conductor [4]. Changing the type of metal coating would not prevent this.

### **Future Directions**

The current priority is to acquire the components and access the equipment necessary to complete the assembly of the device, followed by a full characterization of energy-harvesting performance under full load, and obstruction detection accuracy. Once we have a completed and verified platform, we will send it to our collaborators at the Barrow Neurological Institute (BNI), who will fully characterize the platform in cadavers. From there, we will determine what revisions

will need to be made in future iterations. Afterwards, we must still determine how to evaluate device performance in the long run. In theory, the lifetime of a shunt is on the order of years, and it is critical that we be able to determine the longevity of the device so that we can design it to last equally long. If the device becomes the limiting factor to the shunt's lifetime, then it is highly impractical to integrate such a system into the shunt.

At this time, we intend for a future version to function via NFC rather than RFID because we would like to explore that possibility of allowing the patient to directly assess shunt function using a device such as a smartphone, or a low-cost NFC reader. We would also like to take advantage of the security features enabled by NFC to protect sensitive patient data. BNI has proposed the development of a smartphone application that would allow the patient to log direct measurements of CSF flow and transmit this data back to the healthcare provider. This would allow the provider to have a record of the shunt history and also remotely notify the patient if emergency intervention is necessary.

## REFERENCES

- [1] "Hydrocephalus Fact Sheet", *National Institute of Neurological Disorders and Stroke*, 2013. [Online]. Available: <https://www.ninds.nih.gov/Disorders/Patient-Caregiver-Education/Fact-Sheets/Hydrocephalus-Fact-Sheet>.
- [2] R. Pudenz and E. Foltz, "Hydrocephalus: Overdrainage by ventricular shunts. A review and recommendations", *Surgical Neurology*, vol. 35, no. 3, pp. 200-212, 1991.
- [3] R. Pudenz, "The surgical treatment of hydrocephalus—An historical review", *Surgical Neurology*, vol. 15, no. 1, pp. 15-26, 1981.
- [4] C. Aluise, R. Sowell and D. Butterfield, "Peptides and proteins in plasma and cerebrospinal fluid as biomarkers for the prediction, diagnosis, and monitoring of therapeutic efficacy of Alzheimer's disease", *Biochimica et Biophysica Acta (BBA) - Molecular Basis of Disease*, vol. 1782, no. 10, pp. 549-558, 2008.
- [5] J. Cheatle, A. Bowder, S. Agrawal, M. Sather and L. Hellbusch, "Flow characteristics of cerebrospinal fluid shunt tubing", *Journal of Neurosurgery: Pediatrics*, vol. 9, no. 2, pp. 191-197, 2012.
- [6] B. Warf, "Comparison of 1-year outcomes for the Chhabra and Codman-Hakim Micro Precision shunt systems in Uganda: a prospective study in 195 children", *Journal of Neurosurgery: Pediatrics*, vol. 102, no. 4, pp. 358-362, 2005.
- [7] R. Patwardhan and A. Nanda, "Implanted Ventricular Shunts in the United States: The Billion-dollar-a-year Cost of Hydrocephalus Treatment", *Neurosurgery*, vol. 56, no. 1, pp. 139-145, 2005.
- [8] S. Holland, B. Tighe and P. Gould, "Polymers for biodegradable medical devices. 1. The potential of polyesters as controlled macromolecular release systems", *Journal of Controlled Release*, vol. 4, no. 3, pp. 155-180, 1986.
- [9] T. Babb and W. Kupfer, "Phagocytic and metabolic reactions to chronically implanted metal brain electrodes", *Experimental Neurology*, vol. 86, no. 2, pp. 171-182, 1984.

- [10] D. D. Arumugam, D. W. Engels and M. H. Mickle, "Specific absorption rates in muscle tissues for passive UHF RFID tag backscatter," *2009 IEEE Radio and Wireless Symposium*, San Diego, CA, 2009, pp. 445-448.
- [11] [3]S. Kang, R. Murphy, S. Hwang, S. Lee, D. Harburg, N. Krueger, J. Shin, P. Gamble, H. Cheng, S. Yu, Z. Liu, J. McCall, M. Stephen, H. Ying, J. Kim, G. Park, R. Webb, C. Lee, S. Chung, D. Wie, A. Gujar, B. Vemulapalli, A. Kim, K. Lee, J. Cheng, Y. Huang, S. Lee, P. Braun, W. Ray and J. Rogers, "Bioresorbable silicon electronic sensors for the brain", *Nature*, vol. 530, no. 7588, pp. 71-76, 2016.
- [12] [4]M. Geiger and L. Speckman, "Cerebral Spinal Fluid Flow Sensing Device", US20060020239A1, 2006.
- [13] [5]R. Raj, S. Lakshmanan, D. Apigo, A. Kanwal, S. Liu, T. Russell, J. Madsen, G. Thomas and R. Farrow, "Demonstration that a new flow sensor can operate in the clinical range for cerebrospinal fluid flow", *Sensors and Actuators A: Physical*, vol. 234, pp. 223-231, 2015.
- [14] [6]D. Apigo, P. Bartholomew, T. Russell, A. Kanwal, R. Farrow and G. Thomas, "Evidence of an application of a variable MEMS capacitive sensor for detecting shunt occlusions", *Scientific Reports*, vol. 7, p. 46039, 2017.